

1 **Accelerating Genome- and Phenome-Wide Association Studies using GPUs – A case study**
2 **using data from the Million Veteran Program**

3
4 Alex Rodriguez^{†1}, Youngdae Kim^{‡2}, Tarak Nath Nandi¹, Karl Keat³, Rachit Kumar³, Rohan
5 Bhukar^{4,5}, Mitchell Conery⁶, Molei Liu⁷, John Hessington⁸, Ketan Maheshwari⁹, Drew Schmidt⁹,
6 *VA Million Veteran Program*¹⁰, Edmon Begoli⁹, Georgia Tourassi¹¹, Sumitra Muralidhar¹²,
7 Pradeep Natarajan^{5,13,14,15}, Benjamin F Voight^{1,16,6,17,18}, Kelly Cho^{19,13,20}, J Michael
8 Gaziano^{19,13,20}, Scott M Damrauer^{16,17,21,22}, Katherine P Liao^{23,13,24,25,26}, Wei Zhou^{4,27,28}, Jennifer
9 E Huffman^{23,13,29}, Anurag Verma^{‡16,3,30}, Ravi K Madduri^{‡1}

10
11 ¹Data Science and Learning, Argonne National Laboratory, Lemont, IL, 60439, USA
12 ²Mathematics and Computer Science Division, Argonne National Laboratory, Lemont, IL,
13 60439, USA

14 ³Institute for Biomedical Informatics, University of Pennsylvania - Perelman School of
15 Medicine, Philadelphia, PA, 19104, USA

16 ⁴Program in Medical and Population Genetics, Cambridge, MA, 02142, USA

17 ⁵Cardiovascular Research Center, Massachusetts General Hospital, Boston, MA, 02114, USA

18 ⁶Department of Systems Pharmacology and Translational Therapeutics, University of
19 Pennsylvania - Perelman School of Medicine, Philadelphia, PA, 19104, USA

20 ⁷Department of Biostatistics, Columbia University's Mailman School of Public Health, New
21 York, NY, 10032, USA

22 ⁸Information systems, University of Pennsylvania, Philadelphia, PA, 19104, USA

23 ⁹Oak Ridge National Laboratory, Oak Ridge, TN, USA

24 ¹⁰See Supplement for a list of MVP contributors

25 ¹¹Computing and Computational Sciences Directorate, Oak Ridge National Laboratory, Oak
26 Ridge, TN, 37830, USA

27 ¹²Office of Research and Development, Department of Veterans Affairs, Washington, DC,
28 20420, USA

29 ¹³Department of Medicine, Harvard Medical School, Boston, MA, 02115, USA

30 ¹⁴Program in Medical and Population Genetics and Cardiovascular Disease Initiative, Broad
31 Institute of Harvard and MIT, Cambridge, MA, USA

32 ¹⁵Cardiology Division, Massachusetts General Hospital, Boston, MA, 02114, USA

33 ¹⁶Corporal Michael Crescenz VA Medical Center, Philadelphia, PA, 19104, USA

34 ¹⁷Department of Genetics, University of Pennsylvania - Perelman School of Medicine,
35 Philadelphia, PA, 19104, USA

36 ¹⁸Institute of Translational Medicine and Therapeutics, University of Pennsylvania - Perelman
37 School of Medicine, Philadelphia, PA, 19104, USA

38 ¹⁹MVP Boston Coordinating Center, VA Boston Healthcare System, Boston, MA, 02111, USA

39 ²⁰Department of Medicine, Division of Aging, Brigham and Women's Hospital, Boston, MA,
40 02115, USA

41 ²¹Department of Surgery, University of Pennsylvania - Perelman School of Medicine,
42 Philadelphia, PA, 19104, USA
43 ²²Cardiovascular Institute, University of Pennsylvania - Perelman School of Medicine,
44 Philadelphia, PA, 19104, USA
45 ²³Massachusetts Veterans Epidemiology Research and Information Center (MAVERIC), VA
46 Boston Healthcare System, Boston, MA, 02130, USA
47 ²⁴Department of Biomedical Informatics, Harvard Medical School, Boston, MA, 02115, USA
48 ²⁵Medicine, Rheumatology, VA Boston Healthcare System, Boston, MA, 02130, USA
49 ²⁶Department of Medicine, Division of Rheumatology, Inflammation, and Immunity, Brigham
50 and Women's Hospital, Boston, MA, 02115, USA
51 ²⁷Department of Medicine, Analytic and Translational Genetics Unit, Massachusetts General
52 Hospital, Boston, MA, 02114, USA
53 ²⁸Stanley Center for Psychiatric Research, Cambridge, MA, 02142, USA
54 ²⁹Palo Alto Veterans Institute for Research (PAVIR), Palo Alto Health Care System, Palo Alto,
55 CA, 94304, USA
56 ³⁰Department of Medicine, Division of Translational Medicine and Human Genetics, University
57 of Pennsylvania - Perelman School of Medicine, Philadelphia, PA, 19104, USA
58
59
60
61
62
63
64
65
66
67
68
69
70
71
72
73
74
75
76

77 **Joint Authorship**

78 [†]These authors contributed equally to this work

79 [‡]These authors supervised equally to this work

80 *Corresponding author: Ravi K. Madduri: madduri@anl.gov

81 Abstract

82 The expansion of biobanks has significantly propelled genomic discoveries yet the sheer scale of
83 data within these repositories poses formidable computational hurdles, particularly in handling
84 extensive matrix operations required by prevailing statistical frameworks. In this work, we
85 introduce computational optimizations to the SAIGE (Scalable and Accurate Implementation of
86 Generalized Mixed Model) algorithm, notably employing a GPU-based distributed computing
87 approach to tackle these challenges. We applied these optimizations to conduct a large-scale
88 genome-wide association study (GWAS) across 2,068 phenotypes derived from electronic health
89 records of 635,969 diverse participants from the Veterans Affairs (VA) Million Veteran Program
90 (MVP). Our strategies enabled scaling up the analysis to over 6,000 nodes on the Department of
91 Energy (DOE) Oak Ridge Leadership Computing Facility (OLCF) Summit High-Performance
92 Computer (HPC), resulting in a 20-fold acceleration compared to the baseline model. We also
93 provide a Docker container with our optimizations that was successfully used on multiple cloud
94 infrastructures on UK Biobank and All of Us datasets where we showed significant time and cost
95 benefits over the baseline SAIGE model.

96 Introduction

97

98 The rapid expansion of biobanks has significantly advanced genomic discoveries, facilitating
99 studies on the genetic basis of disease and catalyzing studies in personalized medicine. The
100 increasing number of newly formed biobanks, alongside the continued growth of established
101 ones, enables researchers to conduct studies with increasingly larger sample sizes, yielding more
102 robust and generalizable findings. Furthermore, biobanks linked to electronic health records
103 (EHR) have been instrumental in translational studies, providing data on both the genome and
104 phenotype in large populations (1-7).

105

106 However, the unprecedented size of the data accessible via biobanks require researchers to
107 consider the computational challenges arising from data complexity, analysis methodologies,
108 statistical frameworks, and infrastructure constraints. Addressing the computational limitations
109 requires development of innovative algorithms, optimization strategies, and adaptable computing
110 architectures tailored to the unique requirements of biomedical research. Additionally, fostering
111 collaboration among computational scientists, statisticians, and domain experts proves
112 indispensable in crafting resilient computational tools and workflows capable of facilitating the
113 efficient analysis of burgeoning biobank data. Leveraging the enhanced computational
114 infrastructures afforded by high-performance computing (HPC) and cloud environments further
115 augments the capacity for comprehensive analysis within the biomedical domain.

116

117 One routine statistical analysis that utilizes genetic and phenotypic data available from large
118 biobanks is the genome-wide association study (GWAS). The purpose of GWAS is to identify
119 association between polymorphic DNA variants in the genome among biobank participants and a

120 phenotypic trait or disease of interest, typically extracted from EHR or clinical data from
121 participants where the underlying computation involves millions of iterations of a generalized
122 linear model over the available genetic exposures (8). Furthermore, the complexity of the
123 analysis increases when state-of-the-art approaches extend the analysis to use multi-level models
124 to better account for population architecture and relatedness, in addition to the volume of the data
125 resulting in huge, dense matrix-matrix and matrix-vector operations that are performed as a part
126 of statistical scaffolding (9-12). Compounding this computational complexity are data scaling
127 challenges, including the desire to analyze the entire catalog of traits extracted from EHR data
128 (i.e., the “phenome”, 100s-1000s of traits) and doing so across all population groups represented
129 in order to capture the diverse representation that is increasingly available. The scale of this
130 undertaking requires large amounts of disk space, fast processors, and innovative techniques to
131 take advantage of the resources available.

132
133 The U.S. Department of Veterans Affairs (VA) Million Veteran Program (MVP) stands as a
134 pioneering research endeavor, continually expanding in scope and offering researchers a
135 platform to tackle the aforementioned challenges. This biobank, aimed at advancing precision
136 medicine and improving healthcare outcomes for Veterans, includes a large number of
137 individuals from underrepresented populations. The VA and the Department of Energy (DOE)
138 established an Interagency Agreement (IAA) to combine VA’s vast array of clinical and genomic
139 data with DOE’s national computing capabilities, including the most powerful supercomputer in
140 the Nation, to push the frontiers of precision medicine and computing with vision to improve the
141 lives of Veterans and all Americans and support the national Precision Medicine Initiative. Its
142 primary mission revolves around furnishing comprehensive genotype-phenotype insights into
143 prevalent and significant health outcomes, leveraging the most extensive EHR-linked biobank in
144 the United States. Among the formidable computational challenges encountered in this research
145 is the task of conducting GWAS across a staggering 3.5 billion genetic variants, spanning
146 thousands of traits gleaned from the electronic health records of 635,969 MVP participants.

147
148 SAIGE (the Scalable and Accurate Implementation of Generalized Mixed Model algorithm) (10)
149 is one such state-of-the-art multi-level modeling based GWAS approach designed to
150 accommodate sample relatedness and manage unbalanced case-control ratios typical in biobanks
151 like MVP. A crucial aspect of GWAS analysis entails constructing a Genetic Relationship Matrix
152 (GRM), which measures the genetic relatedness or similarity among individuals within the study
153 cohort. SAIGE offers users the option to generate either a sparse or a full GRM. While a sparse
154 GRM boasts faster executions and lower memory demands, opting for a full GRM provides a
155 more precise assessment of pairwise relatedness among all individuals, enhancing the depiction
156 of genetic relationships. This proves invaluable for various downstream analyses, including
157 estimating heritability, evaluating genetic correlations, and achieving a deeper understanding of
158 the genetic architecture of the trait in question (14). To mitigate the computational burden
159 associated with storing and inverting the full GRM, SAIGE employs the pre-conditioned

160 conjugate gradient (15) method to iteratively solve linear equations. Nevertheless, it still faces
161 substantial computation challenges due to extensive matrix and vector multiplications across
162 numerous iterations.

163
164 In high-performance computing, processors face performance bottlenecks due to memory and
165 disk input/output (I/O) operations. While processors execute computations rapidly, they depend
166 on memory for data storage. Limited memory capacity necessitates frequent reads and writes to
167 disk storage, slowing overall execution. Parallel processing distributes workloads across multiple
168 compute processor units (CPU) but memory limitations persist. These bottlenecks are especially
169 pronounced in large matrix operations. Graphics Processing Units (GPUs) provide an optimized
170 architecture through high memory bandwidth and capacity (16), massive parallelism (17), and
171 reduced data transfer between CPU and memory (18), particularly for large matrix operations.
172 By leveraging these GPU attributes, computationally intensive tasks, like large matrix
173 operations, can experience significant performance enhancements compared to CPU processing
174 alone, mitigating memory and disk I/O bottlenecks.

175
176 We adapted SAIGE, initially tailored for CPU infrastructure, to utilize both CPUs and GPUs at
177 the DOE Oak Ridge Leadership Computing Facility (OLCF) Summit HPC. This adaptation
178 markedly expedited the analysis process, resulting in a more than 20-fold acceleration, far
179 surpassing what would have been attainable on a CPU-based cluster. Furthermore, our work
180 provided a *generic optimization framework* for other analytical tools based on generalized linear
181 mixed models using a full GRM. We also created a Docker container for deployment on various
182 cloud infrastructures. We present a comparison of the time and cost between the SAIGE GPU
183 and CPU versions.

184

185 **Materials and Methods**

186

187 **Study Design, Population Groups, and Phenotypic Definitions**

188 The analysis involved a series of GWAS across 2,068 traits, covering a deep catalog of
189 phenotypes extracted from EHR-derived diagnosis codes, clinical laboratory tests, vital signs,
190 and survey responses. As previously described (13, 19, 20, 21, 22), the analysis was performed
191 using data from 635,969 participants from MVP Genomics Release 4 (23) (**Table 1**) classified
192 into four population groups based on genetic similarity (GIA) to the 1000 Genomes Project (24,
193 25) African (AFR, n = 121,177), Admixed Americans (AMR, n = 59,048), East Asian (EAS, n =
194 6,702), and European (EUR, n = 449,042) superpopulations. After imputation and quality control
195 (QC) filtering, > 44.3M variants (minor allele count (MAC) ≥ 40) were included for analysis. For
196 a visual representation of the analysis, please refer to **Figure 1a**, which illustrates the different
197 quantities for which the analysis was conducted. After trait quality control, 1,854 binary and 214
198 quantitative traits were included in the downstream analysis in at least one population group
199 (**Figure 1b**).

200

201 Additionally, genotype data from the UK Biobank (3) and the All of Us Research Program (7)
202 were utilized to test the software capabilities on a cloud environment. Within the UK Biobank
203 data, we employed the European (EUR, n = 420,500) and African (AFR, n = 6,600) cohorts
204 where PCA was used to measure the population structure (26). The All of Us cohorts included
205 European (EUR, n = 133,000) and African (AFR, n = 55,000) population groups where PCA was
206 used to measure the population structure (7).

207

208 **Biobank-scale genomic analysis across population groups**

209 In total, 4,045 GWAS SAIGE runs were needed for the GW-PheWAS analysis which resulted in
210 over 350 billion variant-trait associations across population groups. The current implementation
211 of the SAIGE algorithm was not analytically tractable at this scale of computation. SAIGE uses
212 R/C++ based tools developed for CPU environments and uses the Intel Threading Building
213 Blocks (TBB) (27) library to enable parallelization. The SAIGE method comprises two primary
214 steps. Step one involves fitting a linear/logistic mixed model with a GRM included under the null
215 hypothesis that no genetic variants are associated with the phenotype of interest. We note that
216 fitting the null mixed model involves thousands of matrix-matrix and matrix-vector operations,
217 which are best suited for a GPU environment. Step two tests each SNP at a time across the
218 genome for their association with the phenotype with a score test using the saddlepoint
219 approximation (SPA) (28) and Firth regression methods (29) to account for unbalanced case-
220 control sample sizes.

221

222 Directly genotyped variants were used for step one of SAIGE and were filtered for pairwise
223 correlation with a window size, number of SNPs and VIF threshold of 50, 5, and 0.2 respectively
224 using Plink1.9 (9). Imputed genetic dosages were used for step two of SAIGE. Only variants
225 with an imputation quality > 0.3 and $MAC \geq 40$ within the relevant population groups were
226 included in the GWAS execution. Analyses were adjusted for age, sex, and the top ten
227 population specific genetic principal components (PC) estimated by Principal component
228 analysis (13).

229 **Computational Infrastructures**

230

231 All GWAS analysis was conducted on the Summit HPC, located at DOE's OLCF. It consists of
232 4,608 nodes, with each node featuring two IBM POWER9 processors and six NVIDIA Tesla
233 V100 GPUs of 16 GB memory. All but 54 of the Summit nodes are equipped with 512 GB of
234 DDR4 memory for the POWER9 processors and 96 GB of high-bandwidth memory (HBM2) for
235 the V100 GPUs. The remaining 54 nodes in Summit HPC are high-memory nodes equipped with
236 2 TB of DDR4 memory for the CPUs and 192 GB of HBM2 for the GPUs with 32 GB of
237 memory per GPU. Specifically, for the GW-PheWAS analysis, we utilized the nodes on Summit
238 with 512 GB DDR4 memory and 96 GB HBM2 memory.

239

240 To further advance the use of SAIGE-GPU in various research environments, we generated
241 Docker and Singularity containers. We conducted extensive testing of this containerized solution
242 on the GPUs available on Google Cloud Platform (GCP) and Azure Cloud Platforms. Our code
243 for containers and optimizations is provided (**Data and materials availability**).
244

245 **Results**

247 We initially focused on optimizing step one for SAIGE as it can largely benefit by using GPUs
248 for matrix-vector operations in the calculation of the GRM on the fly and employed MPI to
249 distribute the data across multiple GPUs. While the standard SAIGE method on CPU-based
250 machines was suitable for relatively small cohorts, it became impractical for larger population
251 groups (e.g., groups similar to 1KG-European and 1KG-Africa in MVP) due to the substantial
252 size of the matrix-vector operations involved. Employing the GPU-modified SAIGE framework,
253 we successfully conducted a total of 4,045 independent GWAS runs. The GWAS analysis was
254 accomplished within 14,286 GPU hours for step one, equivalent to 5 days of wall time, resulting
255 in a 160-fold reduction in required core CPU hours in a CPU environment cluster (**Table 2**). Step
256 two in SAIGE presented distinct challenges due to the need for millions of association tests for
257 each trait, totaling over 3 billion association tests.

258 **Optimizations for SAIGE Step One Using GPUs**

259 The primary challenge we encountered when using the SAIGE algorithm on the DOE OLCF
260 Summit HPC was the IBM POWER9 processors incompatibility with the Intel threading
261 building block (TBB) library, which is instrumental for parallelization within step one. This issue
262 prevented us from installing the native SAIGE version, prompting us to find alternative
263 solutions. In addition, solving the logistic mixed model using the PCG algorithm posed
264 challenges due to the numerous iterations and the time-consuming nature of the process. Step
265 one's time complexity (O) is $O(MN^{1.5})$, where N is the sample size, and M is the number of
266 genetic markers per sample, making the calculation of the GRM a substantial contributor to the
267 overall computational time for this step, particularly when dealing with large sample sizes (as
268 indicated in equations 1, 2, 3) (10). Building and storing the GRM demanded substantial memory
269 and computational resources. SAIGE's approach addressed the memory issue by generating
270 GRM segments on-demand, albeit at the cost of increased time requirements and the need for
271 extensive parallelization using multiple CPUs.

272
273 SAIGE models the relationship between traits (Y) and genotypes (G) while adjusting for other
274 covariates (X) and random genetic effects (b) accounting for unknown sample relatedness based
275 on the linear and logistic mixed models (9) (equation 1):
276

$$277 \logit(Y) = X\alpha + G\beta + b + e \quad (1)$$

278 α and β are the coefficient vectors of fixed effects and genetic effects, respectively and e is a
279 random effect of residual errors. Each element in \mathbf{Y} represents the probability for an individual
280 being a case given the covariates and genotypes as well as the random effect. The variable \mathbf{b} is
281 assumed to be sampled from a normal distribution with a mean of zero, and a standard deviation
282 of $\tau\psi$, where ψ is the GRM calculated as

283
$$\psi = \frac{1}{M} \mathbf{A}^T \mathbf{A} \quad (2)$$

284 where \mathbf{A} is the genotype matrix of size $N \times M$. Optimizing a linear system solution involving the
285 GRM (ψ) matrix on GPUs is our focus.

286
287 The model is fit under the null hypothesis of $\beta = 0$, in which the iterative PCG method is used to
288 obtain a solution to a linear system of equations defined by $\psi\mathbf{x} = \mathbf{b}$ for a given vector b . This
289 iterative process, central to step one, was time-consuming due to multiple matrix-vector
290 operations involving the GRM. Furthermore, building the GRM itself is increasingly memory
291 intensive as the number of individuals and marker panels increase in size. For example, the MVP
292 release 4 population group similar to 1KG-Europeans ($N = 445,444$; $M = 120,000$) would
293 produce a GRM of approximately 800 gigabytes.

294
295 To accelerate the computation time and reduce the memory footprint, we employed distributed
296 computing techniques involving the use of Message Passing Interface (MPI) (30) and were able
297 to successfully exploit the parallel computing capability of GPUs for matrix-vector
298 multiplications. Specifically, we partition the columns of the matrix A that are used to form the
299 GRM and distribute them into a set of nodes on a cluster. For example, node i contains columns
300 $A_{:,s_i:e_i}$ with s_i and e_i denoting the start and end indices of the columns of A stored in node i . At
301 each iteration of the PCG method, a matrix-vector multiplication $\psi\mathbf{v}$ for some vector \mathbf{v} is
302 performed. Using the fact that $\psi\mathbf{v} = \frac{1}{M} \sum_i \mathbf{A}_{:,s_i:e_i} (\mathbf{A}_{:,s_i:e_i}^T \mathbf{v})$, each node computes its summand in
303 parallel on GPUs. The results of all nodes are summed and redistributed using MPI. NVIDIA's
304 BLAS library *cublasgemv* (30) is used to compute the summand to further accelerate the two
305 matrix-vector multiplications, $\mathbf{y}_i := \mathbf{A}_{:,s_i:e_i}^T \mathbf{v}$ and $\mathbf{A}_{:,s_i:e_i} \mathbf{y}_i$, on GPUs (**Figure 2**).

306
307 To deal with the large memory requirement, SAIGE relied on the Intel TBB package to
308 parallelize this step, which was incompatible with the Summit infrastructure. We initially
309 replaced the TBB's parallelization method with OpenMP (32) for executing the matrix-vector
310 operations. However, the primary benefit of accelerating step one lies in the considerably faster
311 matrix computations achieved using GPUs compared to CPUs. We compared the SAIGE version
312 that leveraged OpenMP API for parallelization with the GPU version (**Table 3**) using the
313 Varicose Veins trait (454.1 ICD-9 code). In the OpenMP version, we utilized all 42 available
314 cores on the compute node for parallelizing the matrix calculations to generate the GRM, while
315 for the GPU version we utilized 16 GPUs each equipped with 16 GB of memory in each GPU to

316 distribute subsections of the matrix with dimensions of 8,256 by 445,444. On average, a single
317 PCG iteration on a GPU required approximately 0.069 seconds for the group similar to 1KG-
318 Europe in MVP. In contrast, the OpenMP SAIGE implementation took roughly 5.06 seconds,
319 marking a substantial 72-fold improvement for PCG iterations to converge (**Figure 3**). It took 30
320 minutes (on 3 nodes with 6 GPUs each) using the GPU-SAIGE implementation to complete step
321 one. Conversely, the same analysis conducted with the OpenMP implementation took 4 hours
322 and 8 minutes in a single 42-core node, representing an overall 3-fold improvement and
323 considers other processes within step one such as processing the input data. While the OpenMP
324 implementation successfully executed the calculations in SAIGE step one on CPUs with a low
325 memory footprint, it required numerous CPU parallel processes to achieve convergence. The
326 advantage of using GPUs becomes readily apparent as the genotype matrix size grows, because it
327 takes substantially longer for CPUs to parallelize the matrix operations. The GPU capitalizes on
328 its inherent parallelization capabilities and pre-loading contents of the matrix into memory,
329 offering a substantial performance boost for large-scale genetic analysis.

330
331 It is important to note that, due to computing the complete GRM in parallel GPUs, the memory
332 footprint increased in comparison to the CPU-based approach which processes the GRM in small
333 segments independent of one another. Thus, the number of nodes needed to cover the GPUs is
334 increased per trait in larger population groups. The amount GPUs required for a run was
335 calculated using the formula:

336

$$n_{\text{gpu}} = \text{ceil}(4 \times M \times N / (\text{GPU}_{\text{mem}} * 10^9)) \quad (3)$$

337 This calculation factored in GPU memory capacity (GPU_{mem}), the byte size of a single precision
338 floating-point number (4 bytes), and the conversion between bytes and gigabytes (10^9). This
339 formula can be used for any cohort in additional biobanks to determine the number of GPUs to
340 be used on other computational environments (i.e., cloud infrastructure). This estimation
341 considered the linear relationship between the genotype matrix size, GPU memory available and
342 the required number of nodes which can be visualized (**Figures 4a, 4b**).

343
344 The optimizations made in step one effectively harnessed the speed of GPU matrix computation
345 and parallelization, resulting in a significant reduction in analysis time. The GPU optimization of
346 step one enabled the completion of the GWAS analysis for all traits and population groups
347 within 2,381 node hours, representing a remarkable 20-fold improvement for step one in
348 comparison to the initial native SAIGE implementation in a CPU-based cluster (as presented in
349 **Table 2**). Consequently, step one was accomplished in less than 5 days through efficient
350 utilization of node hours facilitated by high-memory Summit nodes for all MVP traits and
351 population groups. Overall, an effective usage of 22,051 GPUs was needed to complete the
352 analysis.

353
354
355 **SAIGE Step two Job Management**

356 In step two of the SAIGE algorithm, millions of variant association tests were conducted
357 independently, given the highly parallel nature of these jobs. Execution times for both the
358 SAIGE-GPU and SAIGE-OpenMP implementations incorporated these optimizations for step
359 two which showed an improvement of 2 to 3-fold compared to initial tests (as summarized in
360 **Table 4**). To enable parallelization, the MVP genotype data files were partitioned into 219 files
361 based on imputation analysis results. This data partitioning strategy facilitated the parallel
362 execution of 219 jobs per trait and population group, totaling nearly 2 million independent jobs.
363 The predominant challenge in step two revolved around managing the substantial number of jobs
364 required for which we used the R library Tasktools (33), enabling successful submission and
365 monitoring of the jobs.

366

367 **SAIGE-GPU Container on Cloud Infrastructures**

368 While the comprehensive analysis was conducted on the OLCF Summit HPC infrastructure, as
369 the MVP cohort data was exclusively available on OLCF computational resources, we note that
370 other cohorts, such as the United Kingdom Biobank (UKBB) (3) and All of Us Biobank (AoU)
371 (7), can only be accessed through cloud infrastructures like the Google Cloud Platform (GCP)
372 and Azure. In response to this demand, we have developed a specialized container image
373 designed for versatile deployment across various cloud infrastructures.

374 To evaluate its performance, we conducted a comparative study that pitted SAIGE-GPU against
375 SAIGE-CPU using data from the UK and AoU Biobanks. We employed the Type 2 Diabetes
376 (T2D) trait to assess their precision, processing speed, and cost-effectiveness within the GCP
377 cloud environment for two of the largest genetically inferred population groups, namely African
378 and European (**Figure 5** and **Table 5**). For instance, a 5-fold improvement in execution time was
379 seen when analyzing the T2D trait from AoU across the European population group (N =
380 133,000; M = 100,000). Step one completed in 10 minutes using 1 GPU (A100 GPU, 85 GB
381 RAM), whereas the CPU-based SAIGE version consumed 45 minutes on a 64-core virtual
382 machine. Furthermore, the cost of utilizing 1 GPU for the EUR cohort amounted to
383 approximately \$0.42, while the cost of the 64-core VM was \$3.17. A similar trend in terms of
384 cost and time is observed for the AFR population group, which would have a smaller memory
385 footprint due to the matrix size.

386 This same pattern of advantages is evident when applied to UKBB traits, as exemplified in table
387 5. Specifically, we focused on the EUR population group, which consisted of 420,500
388 individuals, closely resembling the MVP EUR cohort in participant size. GCP infrastructure
389 (NVIDIA Tesla A100 GPUs, 12 vCPUs, and 85GB of RAM) was employed to run the T2D trait
390 and completed the analysis in just over 30 minutes, with an average cost of \$1.45. In contrast,
391 utilizing the CPU-based SAIGE version consumed 58 minutes and incurred a cost of \$3.88 using
392 a 96-core VM.

393 **Conclusion**

394

395 We leveraged the GPU computational resources of the DOE OLCF Summit HPC address major
396 computational challenges posed by the increasingly large datasets utilized in genomics research.
397 In this example, we demonstrate optimization of a highly used tool for genomic analyses
398 designed for CPUs, SAIGE. Prior to optimizing step one with GPUs, the analysis would have
399 spanned several years for all genetically inferred population groups. The optimizations have now
400 condensed the completion time to under a month, reducing node hours by a substantial factor.
401 Even though we largely focused on step one of SAIGE, in Step two we showed how we executed
402 millions of variant association tests in parallel, a highly compute-intensive task. We intend to
403 further improve this step by parallelizing this step instead of performing each association in
404 serial mode.

405

406 In a recent article (34), the authors performed a large analysis on over 7,000 traits of the Pan-UK
407 Biobank (35) data for multiple ancestries using hail-batch on the Google Cloud Platform. As
408 previously mentioned, both the European population groups for UKBB and MVP are comparable
409 in size, while the African, Admixed American and Eastern Asian population groups are larger for
410 the MVP. The authors used the SAIGE-CPU implementation to perform close to 300 billion
411 associations and required over 3.8 million CPU hours to complete both step one and step two in
412 SAIGE. In comparison, the MVP analysis required 14,283 GPU hours for step one and
413 approximately 2 million CPU hours for step two to perform over 350 billion associations.

414

415 The MVP has now expanded to a million individuals (36) and plans to collect whole-genome
416 sequencing data, likely to increase the number of low-frequency variants that will be tested in the
417 future. Thus, it is imperative to understand approaches to efficiently optimize software already
418 developed for these data in HPC environments. Our primary focus lay in enhancing the
419 efficiency of SAIGE's first step since it is iteratively employed in numerous downstream SAIGE-
420 related analyses (e.g., SAIGE-GENE (37)). However, our ongoing efforts center on further
421 streamlining SAIGE for GW-PheWAS studies across multiple biobanks such as All of Us, UK
422 Biobank, Penn Medicine BioBank (2).

423

424 The continuous evolution of GPU technology in various implementations offers a promising
425 outlook. The Summit infrastructure currently harnesses NVIDIA CUDA libraries for these
426 operations, but future systems may incorporate different libraries, further accelerating execution
427 times and lowering costs. These systems are expected to feature expanded memory and storage
428 capacities. Additionally, our GPU-based SAIGE implementation can be readily adapted for Intel
429 GPUs using the Intel oneAPI platform and AMD GPUs using their ROCm platform.

430

431 A container is available for deployment on cloud platforms equipped with GPU nodes. The code
432 can be accessed at <https://exascale-genomics.github.io/SAIGE-GPU>. The significant
433 improvements in efficiency achieved with SAIGE using GPUs demonstrate the potential for the

434 development of new and existing tools capable of performing population analysis at the exascale
435 level by optimizing software for GPU usage.
436

437 **References and Notes**

438

- 439 1. B. N. Wolford, C. J. Willer, I. Surakka, Electronic health records: the next wave of complex
440 disease genetics. *Hum. Mol. Genet.* **27**, R14–R21 (2018).
- 441 2. A. Verma, S. M. Damrauer, N. Naseer, J. Weaver, C. M. Kripke, L. Guare, G. Sirugo, R. L.
442 Kember, T. G. Drivas, S. M. Dudek, Y. Bradford, A. Lucas, R. Judy, S. S. Verma, E.
443 Meagher, K. L. Nathanson, M. Feldman, M. D. Ritchie, D. J. Rader, For The Penn Medicine
444 BioBank, The Penn Medicine BioBank: Towards a Genomics-Enabled Learning Healthcare
445 System to Accelerate Precision Medicine in a Diverse Population. *J. Pers. Med.* **12**, 1974
446 (2022).
- 447 3. C. Sudlow, J. Gallacher, N. Allen, V. Beral, P. Burton, J. Danesh, P. Downey, P. Elliott, J.
448 Green, M. Landray, B. Liu, P. Matthews, G. Ong, J. Pell, A. Silman, A. Young, T. Sprosen,
449 T. Peakman, R. Collins, UK biobank: an open access resource for identifying the causes of a
450 wide range of complex diseases of middle and old age. *PLoS Med.* **12**, e1001779 (2015).
- 451 4. M. Zawistowski, L. G. Fritsche, A. Pandit, B. Vanderwerff, S. Patil, E. M. Schmidt, P.
452 VandeHaar, C. J. Willer, C. M. Brummett, S. Kheterpal, X. Zhou, M. Boehnke, G. R.
453 Abecasis, S. Zöllner, The Michigan Genomics Initiative: A biobank linking genotypes and
454 electronic clinical records in Michigan Medicine patients. *Cell Genomics.* **3**, 100257 (2023).
- 455 5. M. I. Kurki, J. Karjalainen, P. Palta, T. P. Sipilä, K. Kristiansson, K. M. Donner, M. P.
456 Reeve, H. Laivuori, M. Aavikko, M. A. Kaunisto, A. Loukola, E. Lahtela, H. Mattsson, P.
457 Laiho, P. Della Briotta Parolo, A. A. Lehisto, M. Kanai, N. Mars, J. Rämö, T. Kiiskinen, H.
458 O. Heyne, K. Veerapen, S. Rüeger, S. Lemmelä, W. Zhou, S. Ruotsalainen, K. Pärn, T.
459 Hiekkalinna, S. Koskelainen, T. Paajanen, V. Llorens, J. Gracia-Tabuenca, H. Siirtola, K.
460 Reis, A. G. Elnahas, B. Sun, C. N. Foley, K. Aalto-Setälä, K. Alasoo, M. Arvas, K. Auro, S.
461 Biswas, A. Bizaki-Vallaskangas, O. Carpen, C.-Y. Chen, O. A. Dada, Z. Ding, M. G. Ehm,
462 K. Eklund, M. Färkkilä, H. Finucane, A. Ganna, A. Ghazal, R. R. Graham, E. M. Green, A.
463 Hakanen, M. Hautalahti, Å. K. Hedman, M. Hiltunen, R. Hinttala, I. Hovatta, X. Hu, A.
464 Huertas-Vazquez, L. Huilaja, J. Hunkapiller, H. Jacob, J.-N. Jensen, H. Joensuu, S. John, V.
465 Julkunen, M. Jung, J. Junntila, K. Kaarniranta, M. Kähönen, R. Kajanne, L. Kallio, R.
466 Kälviäinen, J. Kaprio, FinnGen, N. Kerimov, J. Kettunen, E. Kilpeläinen, T. Kilpi, K.
467 Klinger, V.-M. Kosma, T. Kuopio, V. Kurra, T. Laisk, J. Laukkanen, N. Lawless, A. Liu, S.
468 Longerich, R. Mägi, J. Mäkelä, A. Mäkitie, A. Malarstig, A. Mannermaa, J. Maranville, A.
469 Matakidou, T. Meretoja, S. V. Mozaffari, M. E. K. Niemi, M. Niemi, T. Niiranen, C. J.
470 O'Donnell, M. Obeidat, G. Okafo, H. M. Ollila, A. Palomäki, T. Palotie, J. Partanen, D. S.
471 Paul, M. Pelkonen, R. K. Pendergrass, S. Petrovski, A. Pitkäranta, A. Platt, D. Pulford, E.
472 Punkka, P. Pussinen, N. Raghavan, F. Rahimov, D. Rajpal, N. A. Renaud, B. Riley-Gillis, R.
473 Rodosthenous, E. Saarentaus, A. Salminen, E. Salminen, V. Salomaa, J. Schleutker, R. Serpi,
474 H. Shen, R. Siegel, K. Silander, S. Siltanen, S. Soini, H. Soininen, J. H. Sul, I. Tachmazidou,

475 K. Tasanen, P. Tienari, S. Toppila-Salmi, T. Tukiainen, T. Tuomi, J. A. Turunen, J. C.
476 Ulirsch, F. Vaura, P. Virolainen, J. Waring, D. Waterworth, R. Yang, M. Nelis, A. Reigo, A.
477 Metspalu, L. Milani, T. Esko, C. Fox, A. S. Havulinna, M. Perola, S. Ripatti, A. Jalanko, T.
478 Laitinen, T. P. Mäkelä, R. Plenge, M. McCarthy, H. Runz, M. J. Daly, A. Palotie, FinnGen
479 provides genetic insights from a well-phenotyped isolated population. *Nature*. **613**, 508–518
480 (2023).

481 6. O. Gottesman, H. Kuivaniemi, G. Tromp, W. A. Faustett, R. Li, T. A. Manolio, S. C.
482 Sanderson, J. Kannry, R. Zinberg, M. A. Basford, M. Brilliant, D. J. Carey, R. L. Chisholm,
483 C. G. Chute, J. J. Connolly, D. Crosslin, J. C. Denny, C. J. Gallego, J. L. Haines, H.
484 Hakonarson, J. Harley, G. P. Jarvik, I. Kohane, I. J. Kullo, E. B. Larson, C. McCarty, M. D.
485 Ritchie, D. M. Roden, M. E. Smith, E. P. Böttinger, M. S. Williams, The Electronic Medical
486 Records and Genomics (eMERGE) Network: past, present, and future. *Genet. Med.* **15**, 761–
487 771 (2013).

488 7. The All of Us Research Program Genomics Investigators. Genomic data in the All of Us
489 Research Program. *Nature* (2024). <https://doi.org/10.1038/s41586-023-06957-x>.

490 8. Uffelmann, E., Huang, Q.Q., Munung, N.S. et al. Genome-wide association studies. *Nat Rev*
491 *Methods Primers* **1**, 59 (2021). <https://doi.org/10.1038/s43586-021-00056-9>

492 9. Chang CC, Chow CC, Tellier LC, Vattikuti S, Purcell SM, Lee JJ. Second-generation
493 PLINK: rising to the challenge of larger and richer datasets. *Gigascience*. 2015;4:7.
494 doi:10.1186/s13742-015-0047-8

495 10. W. Zhou, J. B. Nielsen, L. G. Fritsche, R. Dey, M. E. Gabrielsen, B. N. Wolford, J. LeFaive,
496 P. VandeHaar, S. A. Gagliano, A. Gifford, L. A. Bastarache, W.-Q. Wei, J. C. Denny, M.
497 Lin, K. Hveem, H. M. Kang, G. R. Abecasis, C. J. Willer, S. Lee. Efficiently controlling for
498 case-control imbalance and sample relatedness in large-scale genetic association studies. *Nat.*
499 *Genet.* **50**, 1335–1341 (2018).

500 11. Loh PR, Tucker G, Bulik-Sullivan BK, et al. Efficient Bayesian mixed-model analysis
501 increases association power in large cohorts. *Nat Genet*. 2015;47(3):284-290.
502 doi:10.1038/ng.3190

503 12. Mbatchou J, Barnard L, Backman JD, et al. A comparison of methods for correcting for
504 population stratification in genome-wide association studies of rare variants. *Hum Genet*.
505 2019;138(7):749-764. doi:10.1007/s00439-019-02022-3

506 13. A. Verma, J.E. Huffman, A. Rodriguez, M. Conery, M. Liu, Y. Ho, Y. Kim, D. A. Heise, L.
507 Guare, V. A. Panickan, H. Garcon, F. Linares, L. Costa, I. Goethert, R. Tipton, J. Honerlaw,
508 L. Davies, S. Whitbourne, J. Cohen, D.C. Posner, R. Sangar, M. Murray, X. Wang, D.R.
509 Dochtermann, P. Devineni, Y. Shi, T.N. Nandi, T.L. Assimes, C.A. Brunette, R.J. Carroll, R.
510 Clifford, S. Duvall, J. Gelernter, A. Hung, S.K. Iyengar, J. Joseph, R. Kember, H. Kranzler,
511 D. Levey, S. Luoh, V.C. Merritt, C. Overstreet, J.D. Deak, S.F.A. Grant, R. Polimanti, P.
512 Roussos, Y.V. Sun, S. Venkatesh, G. Voloudakis, A. Justice, E. Begoli, R. Ramoni, G.
513 Tourassi, S. Pyarajan, P.S. Tsao, C.J. O'Donnell, S. Muralidhar, J. Moser, J.P. Casas, A. G.
514 Bick, W. Zhou, T. Cai, B. F. Voight, K. Cho, M.J. Gaziano, R.K. Madduri, S.M. Damrauer,

515 K.P. Liao. Diversity and Scale: Genetic Architecture of 2,068 Traits in the VA Million
516 Veteran Program. medRxiv 2023.06.28.23291975; doi:
517 <https://doi.org/10.1101/2023.06.28.23291975>

518 14. Lee, S. H., Yang, J., Goddard, M. E., Visscher, P. M., & Wray, N. R. (2012). Estimation of
519 pleiotropy between complex diseases using single-nucleotide polymorphism-derived
520 genomic relationships and restricted maximum likelihood. *Bioinformatics*, 28(19), 2540-
521 2542.

522 15. Kaasschieter, E. F. Preconditioned conjugate gradients for solving singular systems. *J.*
523 *Comput. Appl. Math.* 24, 265–275 (1988).

524 16. Cook, Shane. Chapter 9 - Optimizing Your Application, In Applications of GPU Computing
525 Series, CUDA Programming. 2013, Pages 305-440, ISBN 9780124159334,
526 <https://doi.org/10.1016/B978-0-12-415933-4.00009-0>

527 17. Baji, T. Evolution of the GPU Device widely used in AI and Massive Parallel Processing,
528 2018 IEEE 2nd Electron Devices Technology and Manufacturing Conference (EDTM),
529 Kobe, Japan, 2018, pp. 7-9, doi: 10.1109/EDTM.2018.8421507.

530 18. N. V. Sunitha, K. Raju and N. N. Chiplunkar, Performance improvement of CUDA
531 applications by reducing CPU-GPU data transfer overhead, 2017 International Conference on
532 Inventive Communication and Computational Technologies (ICICCT), Coimbatore, India,
533 2017, pp. 211-215, doi: 10.1109/ICICCT.2017.7975190.

534 19. J. Honerlaw, Y. Ho, F. Fontin, J. Gosian, M. Maripuri, M. Murray, R. Sangar, A,
535 Galloway, A.J. Zimolzak, S.B. Whitbourne, J.P. Casas, R.B. Ramoni, D.R. Gagnon, T. Cai,
536 K.P. Liao, J.M. Gaziano, S. Muralidhar, K. Cho. Framework of the Centralized Interactive
537 Phenomics Resource (CIPHER) standard for electronic health data-based phenomics
538 knowledgebase, *Journal of the American Medical Informatics Association*, Volume 30, Issue
539 5, May 2023, Pages 958–964, <https://doi.org/10.1093/jamia/ocad030>

540 20. H. Fang, Q. Hui, J. Lynch, J. Honerlaw, T. L. Assimes, J. Huang, M. Vujkovic, S. M.
541 Damrauer, S. Pyarajan, J. M. Gaziano, S. L. DuVall, C. J. O'Donnell, K. Cho, K. Chang, P.
542 W.F. Wilson, P. S. Tsao, R. Ramoni, J. Breeling, G. Huang, S. Muralidhar, J. Moser, S. B.
543 Whitbourne, J. V. Brewer, J. Concato, S. Warren, D. P. Argyres, B. Stephens, M. T. Brophy,
544 D. E. Humphries, N. Do, S. Shayan, X. T. Nguyen, E. Hauser, Y. Sun, H. Zhao, R. McArdle,
545 L. Dellitalia, J. Harley, J. Whittle, J. Beckham, J. Wells, S. Gutierrez, G. Gibson, L.
546 Kaminsky, G. Villareal, S. Kinlay, J. Xu, M. Hamner, K. Sue Haddock, S. Bhushan, P.
547 Iruvanti, M. Godschalk, Z. Ballas, M. Buford, S. Mastorides, J. Klein, N. Ratcliffe, H.
548 Florez, A. Swann, M. Murdoch, P. Sriram, S. S. Yeh, R. Washburn, D. Jhala, S. Aguayo, D.
549 Cohen, S. Sharma, J. Callaghan, K. A. Oursler, M. Whooley, S. Ahuja, A. Gutierrez, R.
550 Schifman, J. Greco, M. Rauchman, R. Servatius, M. Oehlert, A. Wallbom, R. Fernando, T.
551 Morgan, T. Stapley, S. Sherman, G. Anderson, E. Sonel, E. Boyko, L. Meyer, S. Gupta, J.
552 Fayad, A. Hung, J. Lichy, R. Hurley, B. Robey, R. Striker, H. Tang. Harmonizing Genetic
553 Ancestry and Self-identified Race/Ethnicity in Genome-wide Association Studies, *The*
554 *American Journal of Human Genetics*, Volume 105, Issue 4 (2019).

555 21. H. Hunter-Zinck, Y. Shi, M. Li, B. R. Gorman, S.-G. Ji, N. Sun, T. Webster, A. Liem, P.
556 Hsieh, P. Devineni, P. Karnam, X. Gong, L. Radhakrishnan, J. Schmidt, T. L. Assimes, J.
557 Huang, C. Pan, D. Humphries, M. Brophy, J. Moser, S. Muralidhar, G. D. Huang, R.
558 Przygodzki, J. Concato, J. M. Gaziano, J. Gelernter, C. J. O'Donnell, E. R. Hauser, H. Zhao,
559 T. J. O'Leary, VA Million Veteran Program, P. S. Tsao, S. Pyarajan, Genotyping Array
560 Design and Data Quality Control in the Million Veteran Program. *Am. J. Hum. Genet.* 106,
561 535–548 (2020).

562 22. X.-M. T. Nguyen, S. B. Whitbourne, Y. Li, R. M. Quaden, R. J. Song, H.-N. A. Nguyen, K.
563 Harrington, L. Djousse, J. V. V. Brewer, J. Deen, S. Muralidhar, R. B. Ramoni, K. Cho, J. P.
564 Casas, P. S. Tsao, J. M. Gaziano, the VA Million Veteran Program, Data Resource Profile:
565 Self-reported data in the Million Veteran Program: survey development and insights from the
566 first 850 736 participants. *Int. J. Epidemiol.* 52, e1–e17 (2023).

567 23. J. M. Gaziano, J. Concato, M. Brophy, L. Fiore, S. Pyarajan, J. Breeling, S. Whitbourne, J.
568 Deen, C. Shannon, D. Humphries, P. Guarino, M. Aslan, D. Anderson, R. LaFleur, T.
569 Hammond, K. Schaa, J. Moser, G. Huang, S. Muralidhar, R. Przygodzki, T. J. O'Leary,
570 Million Veteran Program: A mega-biobank to study genetic influences on health and disease.
571 *J. Clin. Epidemiol.* 70, 214–223 (2016).

572 24. 1000 Genomes Project Consortium; Auton A, Brooks LD, Durbin RM, Garrison EP, Kang
573 HM, Korbel JO, Marchini JL, McCarthy S, McVean GA, Abecasis GR. A global reference
574 for human genetic variation. *Nature.* 2015 Oct 1;526(7571):68-74. doi: 10.1038/nature15393.
575 PMID: 26432245; PMCID: PMC4750478.

576 25. Committee on the Use of Race, Ethnicity, and Ancestry as Population Descriptors in
577 Genomics Research, Board on Health Sciences Policy, Committee on Population, Health and
578 Medicine Division, Division of Behavioral and Social Sciences and Education, National
579 Academies of Sciences, Engineering, and Medicine, *Using Population Descriptors in
580 Genetics and Genomics Research: A New Framework for an Evolving Field* (National
581 Academies Press, Washington, D.C., 2023; <https://www.nap.edu/catalog/26902>).

582 26. Bycroft C, Freeman C, Petkova D, Band G, Elliott LT, Sharp K, Motyer A, Vukcevic D,
583 Delaneau O, O'Connell J, Cortes A, Welsh S, Young A, Effingham M, McVean G, Leslie S,
584 Allen N, Donnelly P, Marchini J. The UK Biobank resource with deep phenotyping and
585 genomic data. *Nature.* 2018 Oct;562(7726):203-209. doi: 10.1038/s41586-018-0579-z. Epub
586 2018 Oct 10. PMID: 30305743; PMCID: PMC6786975.

587 27. James Reinders. 2007. Intel threading building blocks (First. ed.). O'Reilly & Associates,
588 Inc., USA.

589 28. H. E. Daniels "Saddlepoint Approximations in Statistics," *The Annals of Mathematical
590 Statistics, Ann. Math. Statist.* 25(4), 631-650, (December 1954).

591 29. Firth, D. (1993). Bias reduction of maximum likelihood estimates. *Biometrika*, 80(1), 27–38.
592 DOI: 10.1093/biomet/80.1.27

593 30. Nielsen, Frank (2016). "2. Introduction to MPI: The MessagePassing Interface". *Introduction
594 to HPC with MPI for Data Science.* Springer. pp. 195–211. ISBN 978-3-319-21903-5.

595 31. <https://github.com/clMathLibraries/clBLAS>
596 32. Chandra R, Dagum L, Kohr D, Menon R, Maydan D, McDonald J. Parallel programming in
597 OpenMP. Morgan kaufmann; 2001.
598 33. <https://github.com/RBigData/tasktools>
599 34. Konrad J. Karczewski, Rahul Gupta, Masahiro Kanai, Wenhan Lu, Kristin Tsuo, Ying Wang,
600 Raymond K. Walters, Patrick Turley, Shawneequa Callier, Nikolas Baya, Duncan S. Palmer,
601 Jacqueline I. Goldstein, Gopal Sarma, Matthew Solomonson, Nathan Cheng, Sam Bryant,
602 Claire Churchhouse, Caroline M. Cusick, Timothy Poterba, John Compitello, Daniel King,
603 Wei Zhou, Cotton Seed, Hilary K. Finucane, Mark J. Daly, Benjamin M. Neale, Elizabeth G.
604 Atkinson, Alicia R. Martin Pan-UK Biobank GWAS improves discovery, analysis of genetic
605 architecture, and resolution into ancestry-enriched effects. medRxiv 2024.03.13.24303864;
606 doi: <https://doi.org/10.1101/2024.03.13.24303864>
607 35. <https://pan.ukbb.broadinstitute.org/>
608 36. Kolata, G. (2023, November 15). V.A. Recruits Millionth Veteran for its Genetic Research
609 Database. The New York Times. <https://www.nytimes.com/2023/11/15/health/million-veterans-database-va.html>
610 37. Zhou, W., Bi, W., Zhao, Z. et al. SAIGE-GENE+ improves the efficiency and accuracy of
611 set-based rare variant association tests. Nat Genet 54, 1466–1469 (2022).
612 <https://doi.org/10.1038/s41588-022-01178-w>
613

614 615 Acknowledgments

616
617 We thank the Million Veteran Program, Office of Research and Development, and Veterans Health
618 Administration for supporting this work. We would like to sincerely thank Dr. Thomas Zacharia for
619 providing access to the supercomputers at the Oak Ridge National Laboratory Leadership Computing
620 Facility and Dr. Dimitri Kusenov, the previous DOE Headquarters lead for the VA-DOE partnership, for
621 his invaluable guidance and support. Their contributions have been instrumental in the successful
622 completion of this study. Last but not least, we thank former staff members, and volunteers, who have
623 contributed to MVP and, most of all, MVP participants for their service and their continued contributions
624 to our nation through participation in this study. This publication does not represent the views of the
625 Department of Veteran Affairs or the United States Government.
626

627 Funding

628 The work was supported by the Million Veteran Program award #MVP000. This research used resources
629 from the Knowledge Discovery Infrastructure at the Oak Ridge National Laboratory, supported by the
630 Office of Science of the U.S. Department of Energy under Contract No. DE-AC05-00OR22725 and the
631 Department of Veterans Affairs Office of Information Technology Inter-Agency Agreement with the
632 Department of Energy under IAA No. VA118-16-M-1062. Other support by the National Institute of
633 General Medical Sciences grant R01GM138597 (AV); National Institute Health grant T32 AA028259
634 (JDD); National Library of Medicine Grant 5R01LM010685 (RJC); National Human Genome Research
635 Institute grant K99HG012222 (WZ); National Institute of Arthritis and Musculoskeletal and Skin
636 Diseases grant P30AR072577 (KPL); National Institute of Diabetes and Digestive and Kidney Diseases

637 grant DK126194 (BFV); National Institute of Health grants NIR01AG067025, K08MH122911 (GV);
638 National Institute of Health grants BX004189, R01AG065582, R01AG067025 (PR); Office of Research
639 and Development, Veterans Health Administration award I01CX001849-01 (JG); Office of Research and
640 Development, Veterans Health Administration awards BX004821, CX001737, BX005831 (YSV);
641 Veterans Health Administration awards IK2-CX001780 (SMD).

642

643 **Author contributions**

644

645 **Conceptualization:** AAR, YK, TNN, KK, RB, JEH, MC, ML, KM, JH, DS, EB, GT, SM, KC, MJG,
646 BFV, SD, KPL, WZ, AV, RKM; **Methodology:** AAR, YK, TNN, KK, RB, JEH, MC, ML, KM, JH, DS,
647 BFV, SD, KPL, WZ, AV, RKM; **Investigation:** AAR, YK, TNN, KK, RB, JEH, MC, ML, KM, JH, DS,
648 MC, SM, BFV, KC, MJG, SD, KPL, WZ, AV, RKM; **Visualization:** AAR, YK, TNN, KK, JEH, MC,
649 SM, BFV, KC, MJG, SD, KPL, WZ, AV, RKM; **Funding acquisition:** EB, GT, PN, SM, KC, MJG, SD,
650 KPL, AV, RKM; **Project administration:** AAR, JEH, MJG, SD, KPL, WZ, AV, RKM; **Supervision:**
651 EB, GT, SM, PN, AV, MJG, SD, KPL, RKM; **Writing – original draft:** AAR, YK, TNN, KK, RB, JEH,
652 AV, WZ, RKM; **Writing – review & editing:** AAR, YK, TNN, KK, RB, JEH, MC, ML, SM, BFV, KC,
653 MJG, SD, KPL, WZ, AV, RKM.

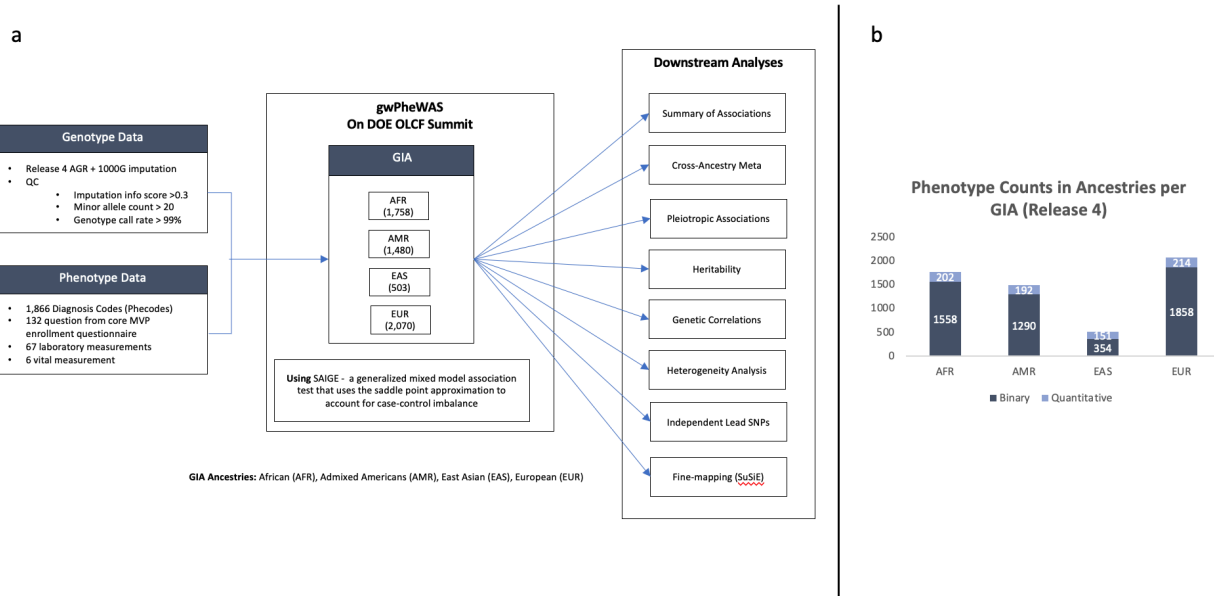
654

655 **Data and materials availability**

656 The optimized SAIGE-GPU software can be accessed at the GitHub page <https://exascale->
657 [genomics.github.io/SAIGE-GPU](https://exascale-genomics.github.io/SAIGE-GPU).

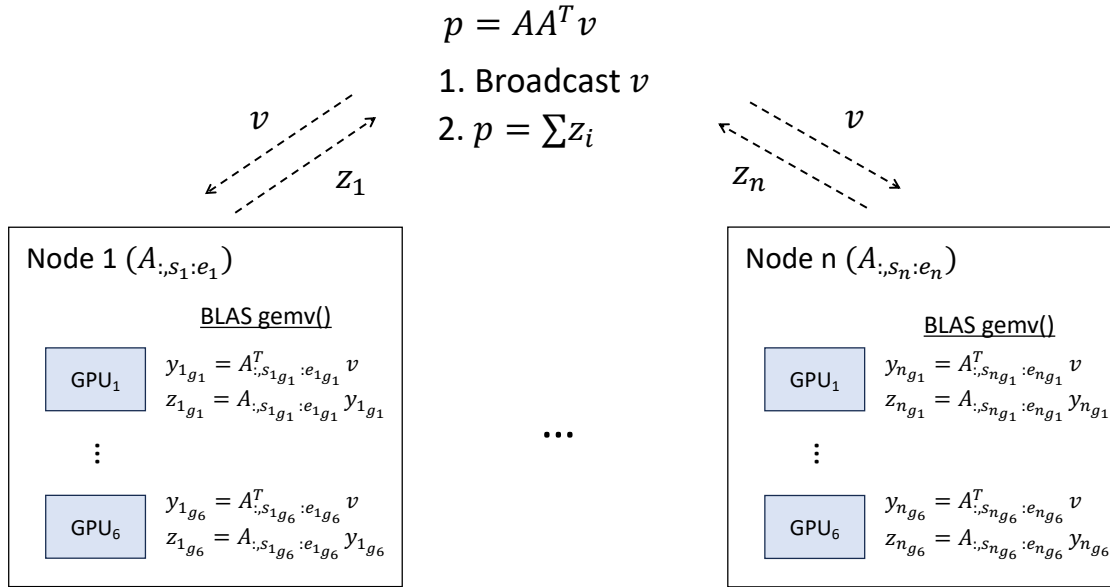
658

659



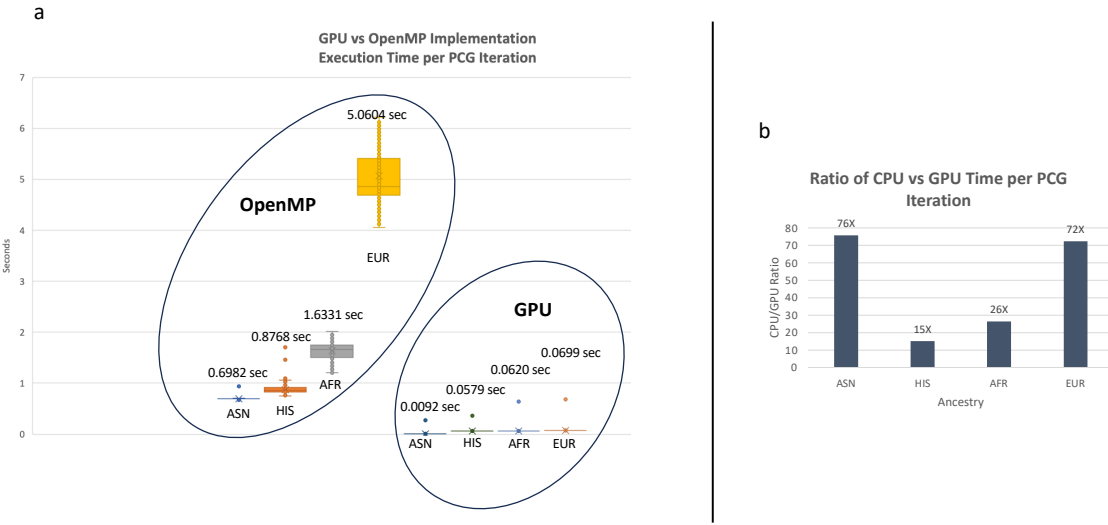
660

661 **Fig. 1** Overview of genomic analysis in multiple population groups. a) Schematic representation
662 illustrating the diverse set of GIA population groups. The analysis covers a deep catalog of traits
663 extracted from electronic health records, clinical laboratory tests, vital signs, and survey
664 responses. b) Chart categorizing traits into binary or quantitative types across different
665 population groups. The height of each bar corresponds to the number of traits in each category,
666 providing an overview of the trait composition for subsequent genomic analyses.
667

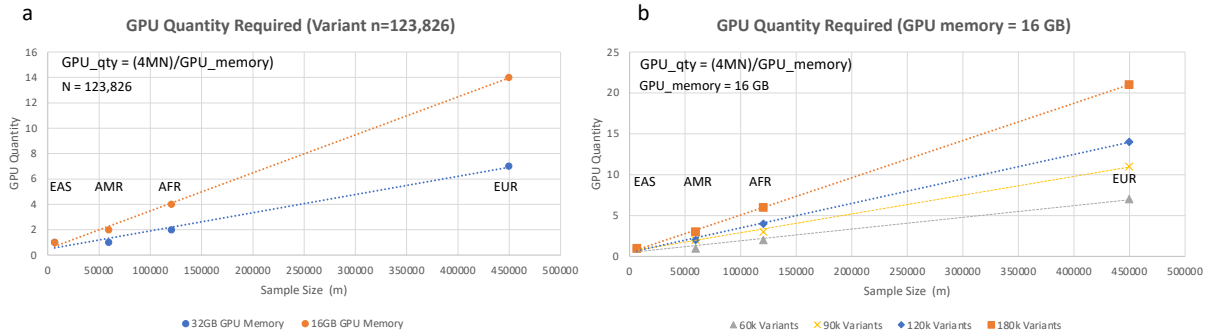


668
669
670
671
672
673
674

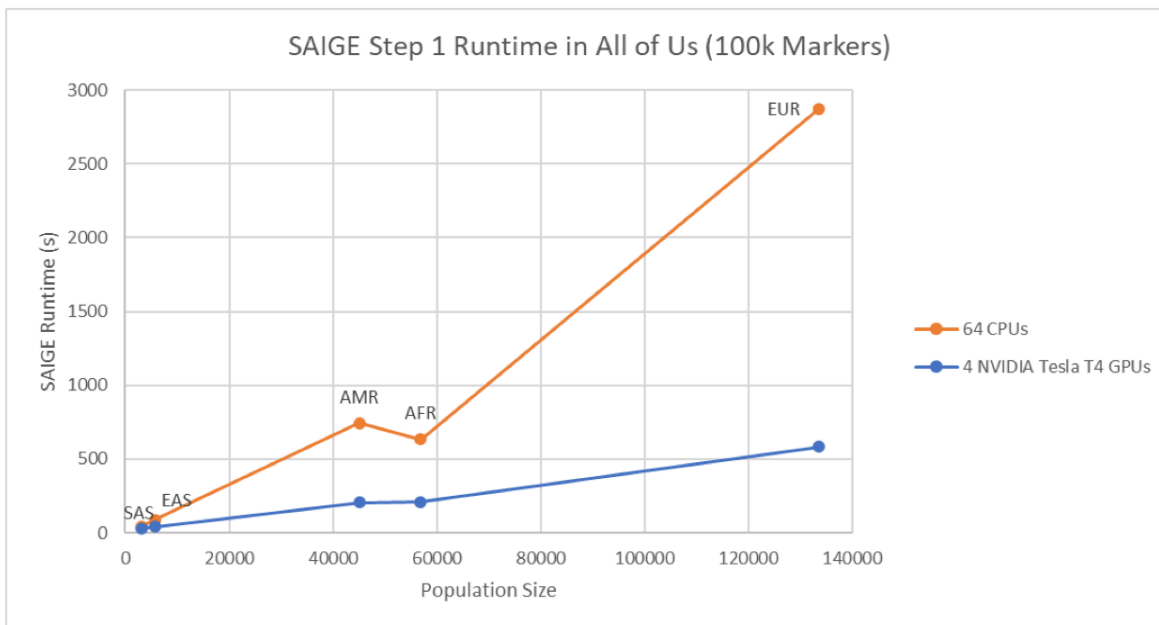
Fig. 2 Distributed BLAS gemv(), matrix-vector multiplication, using GPUs on the cluster. The columns of matrix A are distributed and preloaded on GPUs, with node i having columns with indices from s_i to e_i , and these columns are distributed on GPUs on that node. To compute $p = AA^T v$, we first broadcast v to GPUs, and each node computes a partial solution on GPUs. These partial solutions are aggregated to compute a solution p .



675
676 **Fig. 3** Comparative Performance of GPU and CPU Implementations in SAIGE Step one - This
677 figure compares the execution time for each iteration of matrix operations in SAIGE Step one for
678 the European population group. a) Demonstration of the time required for a single PCG iteration
679 on a GPU, showcasing the efficient parallelization within the GPU. b) Contrast with the OpenMP
680 implementation on CPUs, emphasizing the significant speed improvement achieved with GPU
681 acceleration. As the genotype matrix size increases, the advantage of using the GPU version
682 becomes more pronounced, as highlighted by the diminishing execution time on the GPU
683 compared to the CPU.



684
685 **Fig. 4** GPU Node Requirements and Memory Impact – GPU node requirement highlight the
686 linear relationship between genotype matrix size and the required number of nodes, offering
687 insights into efficient GPU utilization. The GPU node requirement factored in the GPU memory,
688 the byte size of a single precision floating-point number, and the conversion between bytes and
689 gigabytes. A) Impact of changing the memory available in the GPU. B) Impact of changing
690 number of genotype variants in the input matrix and fixing the GPU memory to 16 gigabytes per
691 GPU, emphasizing considerations for diverse biobank cohorts and computational environments.
692



693
694 **Fig. 5** SAIGE step one run time for All of Us data. The figure shows the time comparison of
695 running SAIGE step one for the T2D phenotype on the Google Cloud Platform for the 5
696 population groups (EUR, AFR, AMR, EAS, SAS). The analysis was executed on 4 NVIDIA T4
697 GPUs for the SAIGE-GPU version and a 64-CPU VM for the SAIGE-CPU version.
698

699

Population Group	Participants (Release 4)
AFR	121,177
AMR	59,048
EAS	6,702
EUR	449,042

700

701

702 **Table 1** Participant quantity in each grouping method per population group. Data was made
703 available on OLCF Summit HPC to perform a GWAS analysis for all traits analysis and all
704 population groups.

705

706

Population Group	Trait Quantity	Step One CPU hours for all traits (Projected)		Step One GPU hours for all traits (Production)
		Native SAIGE	SAIGE-OpenMP	
AFR	1,760	322,768	78,266	1,336
AMR	1,482	72,284	60,295	411
EAS	505	27,162	12,253	116
EUR	2,072	1,371,960	330,372	12,420
Total	5,819	1,794,714	481,186	14,283

707

708 **Table 2** Projection times to complete GWAS for all traits (5,819) using SAIGE step one using
709 the different implementations of SAIGE: Native, OpenMP and GPU versions on CPU and GPU
710 environments.

711

712

Population Group	Subjects	Step one for Varicose Veins (hours)		
		Native SAIGE	SAIGE-OpenMP	SAIGE-GPU
AFR	121,725	5.10	1.06	0.38
AMR	51,124	1.50	0.97	0.28
EAS	8,003	0.97	0.58	0.23
EUR	458,307	25.75	4.10	1.50

713

714

715 **Table 3** Execution times for SAIGE step one on Varicose Veins (ICD-9 code 454.1) using 3
716 versions of the SAIGE algorithm on the different OLCF infrastructures. CPU environment
717 contained 32-core nodes, while the GPU nodes contain 42-cores and GPUs with 32 GB of RAM.
718

719

720

Step two for all traits (hours)						
Population Group	Trait Quantity	CPU Environment		GPU Environment		Fold-Change
		Hours for a Single Trait	Projection for all traits	Single Trait	Production run for all traits	
AFR	1,760	446	784,960	254	397,428	1.98
AMR	1,482	228	337,896	146	214,353	1.58
EAS	505	59	29,795	50	22,724	1.31
EUR	2,072	1,209	2,505,048	359	1,397,606	1.79
Total	5,819	1,942	3,657,699	809	2,032,111	1.80

721

722 **Table 4** Execution time for SAIGE step two on Varicose Veins (PheCode 454.1) using 2
723 versions of the SAIGE algorithm on a CPU and GPU environment.

724

725

Category	All of Us		UK Biobank	
	European ⁺	African American ⁺	European ⁺	African ⁺
Variant Size	100,000	100,000	100,000	100,000
Sample Size	133,000	55,000	420,500	6,600
SAIGE GPU Analysis Time (hours)*	0.16	0.1	0.55	0.02
SAIGE GPU Analysis Cost	\$0.42	\$0.26	\$1.45	\$0.05
SAIGE CPU Analysis Time (hours)**	0.8	0.17	0.98	0.25
SAIGE CPU Analysis Cost	\$3.17	\$0.67	\$3.88	\$0.99

726

727 * Google Cloud - A100 GPU, 85 GB RAM, \$2.64/hour

728 ** Google Cloud - 96 Core VM, \$3.96/hour

729 + Phenotype used was Type 2 Diabetes

730

731 **Table 5** Cost and time execution comparison using All of Us and UK Biobank data on Google
732 Cloud Platform for SAIGE-GPU version vs the native SAIGE version.

733